

Dynamics of Hingeless Rotor Blade by Varying Lay-Up Scheme

Suvanit Chitsiriphanit

Department of Mechanical and Aerospace Engineering, Faculty of Engineering,
King Mongkut's University of Technology North Bangkok, Bangkok, Thailand 10800
Corresponding Author: suvanitc@kmutnb.ac.th, Tel: 02 9132500, Fax: 02 5869541

Abstract

Composite material has been widely used as important constituents of structure due to high strength to weight ratio. This paper presents the study of composite rotor blade (S2Glass/Epoxy, Kev49/Epoxy and AS4/3501-6) with the following stacking sequences: $[\pm 45/0_3]_s$, $[90/0/\pm 45/0]_s$ and $[\pm 45/0/90]_s$. The results in terms of mode shapes and frequencies are obtained via computer simulation. It is found that the first 6 modes of vibrations consist of three flapwise modes, two edgewise modes and one torsion mode. Furthermore, the constraining effect on rotor blade is examined by adding boundary condition at Δ_1 and Δ_2 respectively. It can affect the change of blade frequency. The results show that the most increment of frequency is the 2nd mode for all laminates as the frequency of the 5th mode is no more than 5% increase for the $[\pm 45/0/90]_s$ and $[90/0/\pm 45/0]_s$ laminates.

Keywords: Composite material, Frequency and Mechanical vibration

1. Introduction

One of the primary concerns in composite blade is the vibration, which may affect the fatigue life of mechanical components and increase noise. It is based on the fact that composite rotor blade has been widely used in industry such as helicopter blade [1-5] and wind turbine due to the flexibility and lightweight configuration. Composite materials have high fatigue resistance on a stress basis. Stacking sequences and fiber directions can be tailored to optimize the strength of structure. In general, the unwanted vibration and resonance problems can cause the bending of structures and lead to high

stresses and strains in structural material. The purpose of this paper is to study the free vibration of the composite blade under variation of constraints. Due to the complexity of composite structure, the numerical method was employed to obtain the results in terms of mode shapes and blade frequencies [5]. There are some existing literature [6-9] showed that low frequency sound can produce annoyance and cause adverse health effects in sensitive people. The noise produced by these rotor blades can be diminished as the technology has improved. As blade configurations have become more efficient, less energy is converted into acoustic energy.

2. Vibrations of Continuous System

Vibrations are of great importance in a variety of applications. An analysis of the blade vibration can be depicted in Fig. 1.

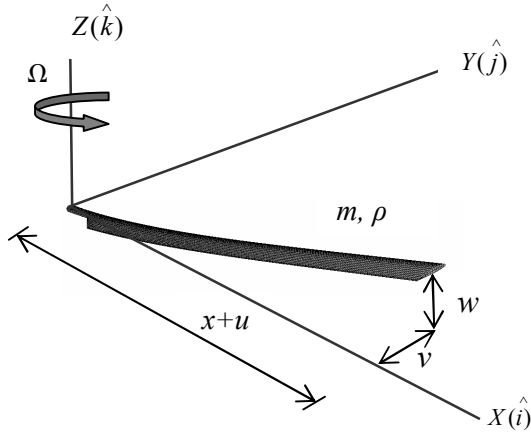


Fig. 1 Schematic of blade deformation

Considering the deformation of rotating blade, which is initially straight, is in its deformed state. The velocity of blade can be expressed as

$$\tilde{V} = \frac{d\tilde{R}}{dt} + \tilde{\omega} \times \tilde{R} \quad (1)$$

$$\tilde{V} = [\dot{u} - (y+v)\Omega]\hat{i} + [\dot{v} + (x+u)\Omega]\hat{j} + \dot{w}\hat{k} \quad (2)$$

where $\tilde{\omega}$ and Ω are the angular velocity, \tilde{R} is the position vector and $(u, v$ and $w)$ are the displacements. To obtain the motion of rotor blade, the strain energy (U) and kinetic energy (T) are determined by the following expressions

$$U = \frac{E}{2} \iiint_V \varepsilon_{xx}^2 dx dy dz \quad (3)$$

in which E is the elastic modulus and ε_{xx} is the axial strain in the x - direction. To calculate the kinetic energy of system, Eq. (2) is substituted into Eq. (4)

$$T = \frac{1}{2} \iiint_V \rho \tilde{V} \cdot \tilde{V} dx dy dz \quad (4)$$

Axial force $F(x)$ in the x - direction due to the inertial mass is defined by Eqs. (5) - (6)

$$F(x) = EA \frac{\partial u}{\partial x} = \int_x^L m \Omega^2 \mu d\mu \quad (5)$$

$$m = \rho dy dz \quad (6)$$

where ρ is the density, m is the mass per unit length and μ is the radial distance from z axis.

The equation of blade motion can be obtained by substituting Eqs. (2) - (6) into the Hamilton's principle. Due to the complexity of a composite blade, the analytical approach is impractical. Hence, finite element method [10] was employed in this research. The blade was discretized into shell elements, each with 6 nodal degrees of freedom. Based on this method, the systems of structure are composed of the elemental stiffness matrix $[K]$, the elemental mass matrix $[M]$ and the elemental load vector $\{F\}$. The dimensions of these matrices depend on the characteristics of blade. The equation of motion can be defined as

$$[M]\{\ddot{q}\} + [K]\{q\} = \{F\} \quad (7)$$

where $\{q\}$ is the vector of generalized coordinates.

The treatment given in this study will be restricted to the free vibration [11]. To study the natural frequency, eigenvalue and eigenvector can be obtained by neglecting the load vector in Eq. (7)

$$[M]\{\ddot{q}\} + [K]\{q\} = 0 \quad (8)$$

Assuming simple harmonic motion for generalized displacement

$$q(t) = \bar{q} e^{i\omega t} \quad (9)$$

where ω is the frequency of the system and $\{\bar{q}\}$ is the eigenvector corresponding to its frequency. Eq. (8) can be rewritten as

$$[[K] - \omega^2 [M]]\{\bar{q}\} = 0 \quad (10)$$

Eq. (10) will be used to extract the eigenvalue and corresponding eigenvector of the systems. Generally, the numerous results can be obtained from this method. However, this work is of interest in low frequency of blade vibration. The

details of composite blade will be described in the following section.

3. Composite Materials

The principal reinforcement fibers used in this research are carbon (graphite), glass and aramid (kevlar) fibers. The typical properties of these fibers can be described as follows: 1). Carbon fiber offers excellent stiffness and strength property. They are manufactured from a variety of starting material fibers. Most of the graphite fibers that are commercially available range in diameter 0.3 to 0.5 millimeters. 2). Glass fibers are still the most popular reinforcement materials for making composites due to their low cost and high strength. In particular, S glass fibers (magnesium aluminosilicate) offer high tensile strength and better properties at elevated temperatures. The diameters of the glass fibers range from 0.1 to 0.8 millimeters. 3). Aramid fibers are the generic name for fibers formed from polymers. Kevlar fibers are light and possess very high strength and rather high modulus. For matrix, epoxy resins used in forming composites are compatible with all types of fibers and are used for the majority of advanced composite materials. The tensile strength of epoxy can be as high as 60 MPa and the modulus greater than 3.45 GPa.

In principle, laminae with various fiber orientations are combined together to form laminated composite. A laminate consists of a number of different fiber orientations. Each lamina may contain one or more plies of the same fiber direction. The laminate properties depend on the lamina fiber orientation as well as its position in the laminate (the stacking sequence). The symmetric lay-up was used in this work.

According to the plate constitutive equations, the stiffness matrix of blade shell can be defined as

$$\text{Stiffness matrix} = \begin{bmatrix} A & B \\ B & D \end{bmatrix} \quad (11)$$

$$(A_{ij}, B_{ij}, D_{ij}) = \int_{-h/2}^{h/2} \bar{Q}_{ij}^{(k)} (1, z, z^2) dz \quad (12)$$

$$A_{ij} = \sum_{k=1}^n \bar{Q}_{ij}^{(k)} t_k \quad (13)$$

$$B_{ij} = \sum_{k=1}^n \bar{Q}_{ij}^{(k)} t_k \bar{z}_k \quad (14)$$

$$D_{ij} = \sum_{k=1}^n \bar{Q}_{ij}^{(k)} \left(t_k \bar{z}_k^2 + \frac{t_k^3}{12} \right) \quad (15)$$

where coefficients A_{ij} , B_{ij} and D_{ij} are extensional, coupling and bending stiffness respectively, h is the thickness of the plate and n is the number of layers in the laminate. The thickness and the distance to the centroid of the k^{th} lamina are denoted by t_k and \bar{z}_k respectively.

4. Research Procedure

Lightweight configuration of blade was constructed of composite materials and analyzed by computer using finite element method. The mechanical properties of composite materials: (S2Glass/Epoxy, Kev49/Epoxy and AS4/3501-6), which are necessary for a blade model, are summarized into tabular form as listed in Table. 1. Table. 1 Mechanical properties of composite materials [12,13]

Composite materials	S2Glass /Epoxy	Kev49 /Epoxy	AS4 /3501-6
E_1 (GPa)	43.3	87	140
E_2 (GPa)	12.7	5.5	10
$G_{12} = G_{13}$ (GPa)	4.5	2.2	7
G_{23} (GPa)	3.2	1.57	5
ν_{12}	0.29	0.34	0.30
ρ (g / cm ³)	1.80	1.40	1.55

The whole blade was made of individual composite materials as given in Table. 1. The symmetric lay-ups of $[\pm 45/0_3]_s$, $[90/0/\pm 45/0]_s$ and $[\pm 45/0/90]_s$ were used as blade shell.

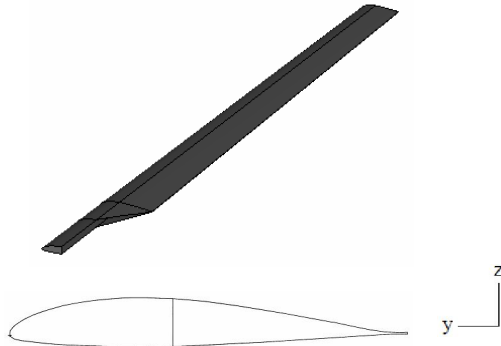


Fig. 2 Two-cell unsymmetrical cross section

The blade configurations such as chord length and span are shown in Figs. 2 - 3. The chord is 0.4 meters in length, the span of blade (L) is 2.64 meters in length and the skin thickness of composite blade is 9 millimeters approximately. The planform of the composite blade with two-cell cross section was modeled using ABAQUS [14] and then discretized into 44,610 biquadratic plane stress elements (CPS8), which have 8 nodes. Each node of element has 6 degrees of freedom ($u, v, w, \theta_x, \theta_y$ and θ_z). Where (u, v and w) are the displacement degrees of freedom and (θ_x, θ_y and θ_z) are the rotational degrees of freedom.

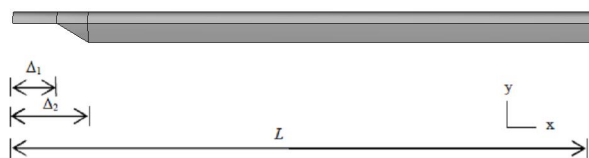


Fig. 3 Boundary conditions at Δ_1 and Δ_2

It can be seen in Fig. 3 that Δ_i denotes the distance between the rotor hub and the additional boundary condition in order to study the effect of

constraint. The degrees of freedom (u, v and w) at the constraining point were set to zero. The ratio L/Δ_1 is 13.25 and L/Δ_2 is 7.75 with $\Delta_1 = 0.20$ meters and $\Delta_2 = 0.34$ meters respectively. For the case of Δ_0 , the blade shell was clamped to the hub center ($x = 0$ meters) and all degrees of freedom ($u, v, w, \theta_x, \theta_y$ and θ_z) were constrained. The simulation results will be described in the next section.

5. Results of Computer Simulation

To study the blade vibration, the model was developed as mentioned in the previous section. There are two parts of simulation results obtained from numerical method. Since this study is of interest in low frequencies, the first 6 mode shapes and frequencies will be presented.

5.1 Mode shape

Results in terms of various mode shapes under boundary condition (Δ_0) in the range of low frequency are demonstrated as follows:



F1: First flapwise mode



E1: First edgewise mode



F2: Second flapwise mode

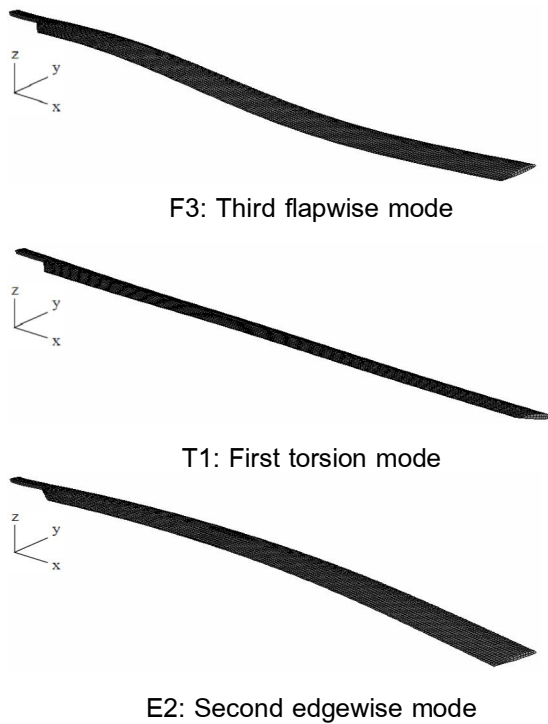


Fig. 4 The first 6 modes of composite blade

It is evident from Fig. 4 that the first 6 modes appear in the following order: F1:First flapwise mode, E1:First edgewise mode, F2:Second flapwise mode, F3:Third flapwise mode, T1:First torsion mode and E2:Second edgewise mode.

5.2 Frequency

For resulting frequencies, Figs. 5-7 show the three different sets of blade frequencies corresponding to three stacking sequences for each type of composite material.

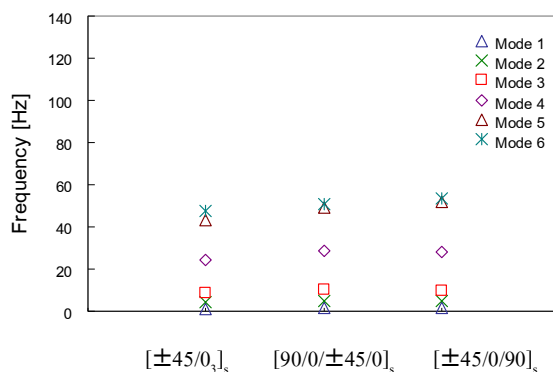


Fig. 5 Natural frequency of S2Glass/Epoxy

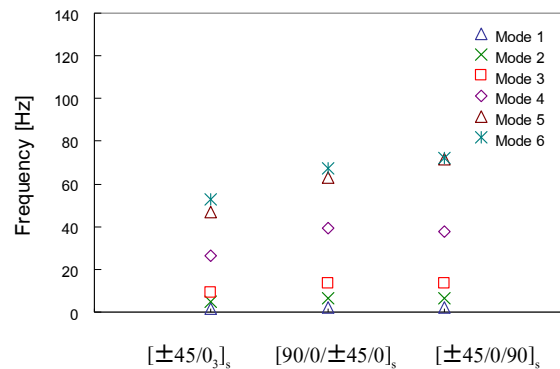


Fig. 6 Natural frequency of Kev49/Epoxy

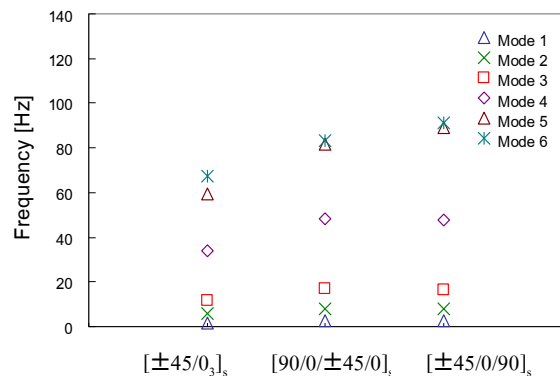


Fig. 7 Natural frequency of AS4/3501-6

Simulation results illustrate that blade natural frequencies have similar trend for all three types of composite materials. It can be observed that frequencies keep increasing from the symmetric lay-ups of $[\pm 45/0]_s$, $[90/0/\pm 45/0]_s$ and $[\pm 45/0/90]_s$ by comparing individual mode.

5.3 Results of constraining effect

In this section, the constraining effect was investigated by adding boundary condition away from rotor hub at $\Delta_1 = 0.2$ meters and $\Delta_2 = 0.34$ meters respectively as shown in Fig. 3. As mentioned earlier, the degrees of freedom (u , v and w) at this constraining point were set to zero. The normalized frequency (f/f_0) defined as frequency for each case divided by its normal mode is illustrated in Figs. 8-10.

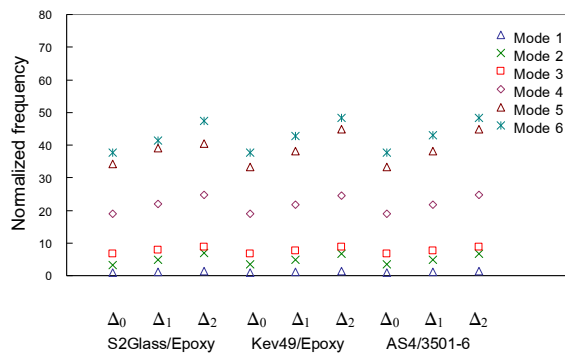


Fig. 8 Normalized frequency (f/f_0)
in case of $[\pm 45/0_3]_s$ laminates

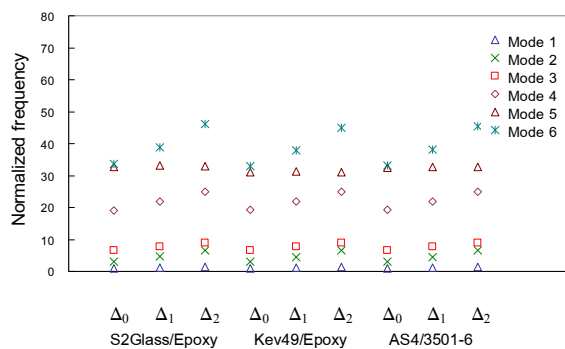


Fig. 9 Normalized frequency (f/f_0)
in case of $[90/0/\pm 45/0]_s$ laminates

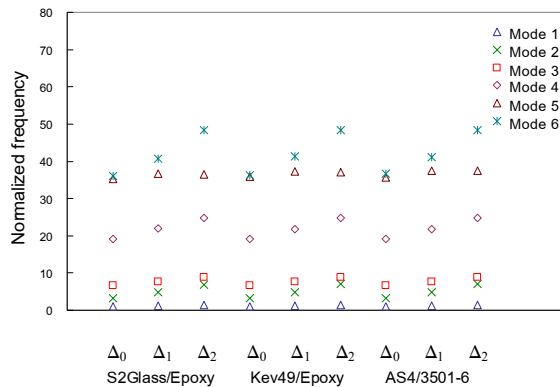


Fig. 10 Normalized frequency (f/f_0)
in case of $[\pm 45/0/90]_s$ laminates

It is apparent that the normalized frequencies (f/f_0) vary as the boundary condition is added from Δ_0 , Δ_1 and Δ_2 respectively. In case of the blade shell with the lay-up of $[\pm 45/0_3]_s$, the increment of frequency becomes greater starting

from the 4th mode. Contrary to the $[\pm 45/0/90]_s$ and $[90/0/\pm 45/0]_s$ laminates, the constraints have minimal effect on the 5th mode. The percent increase of frequency produced by attaching boundary conditions at the distance of (Δ_1) and (Δ_2) on a composite blade can be seen in Table. 2 and 3 respectively.

Table. 2 Comparison of percent increase of frequency in case of the ratio $L/\Delta_1 = 13.25$

Mode	1	2	3	4	5	6
S2Glass/Epoxy						
$[\pm 45/0_3]_s$	21.7	47.7	16.5	14.8	13.7	10.3
$[90/0/\pm 45/0]_s$	21.5	50.6	16.2	14.6	1.0	14.9
$[\pm 45/0/90]_s$	21.4	53.3	16.2	14.6	4.0	12.9
Kev49/Epoxy						
$[\pm 45/0_3]_s$	21.5	42.5	16.6	15.0	14.3	14.1
$[90/0/\pm 45/0]_s$	21.4	48.2	16.0	14.5	1.0	14.5
$[\pm 45/0/90]_s$	21.2	52.8	16.1	14.6	3.8	13.7
AS4/3501-6						
$[\pm 45/0_3]_s$	21.7	43.3	16.7	15.0	14.4	14.1
$[90/0/\pm 45/0]_s$	21.6	49.1	16.2	14.6	1.0	14.8
$[\pm 45/0/90]_s$	21.3	53.2	16.1	14.6	5.0	12.4

Significant change of blade frequencies can be observed between the blade's flapwise, edgewise, and torsion mode as listed in Table. 2 and 3. It can be noted from Table. 2 that the shifts in frequency of different composite blade under constraining effect have similar trend. That is, the blade frequencies keep increasing for all laminates. The increasing frequencies of mode 1, 3, 4 and 6 are within the range of 22% and the frequency of the 2nd mode increases to approximately 50% as the 5th mode is no more than 5% increasing frequency for $[\pm 45/0/90]_s$ and $[90/0/\pm 45/0]_s$ laminates.

Table. 3 Comparison of percent increase of frequency in case of the ratio $L / \Delta_2 = 7.75$

Mode	1	2	3	4	5	6
S2Glass/Epoxy						
$[\pm 45/0_3]_s$	39.3	109	32.3	29.8	18.4	26.1
$[90/0/\pm 45/0]_s$	40.0	116	32.4	29.8	0.6	36.8
$[\pm 45/0/90]_s$	39.4	120	32.1	29.7	3.6	34.4
Kev49/Epoxy						
$[\pm 45/0_3]_s$	38.4	98.3	32.1	29.8	34.7	28.4
$[90/0/\pm 45/0]_s$	40.0	112	32.4	29.8	0.5	36.4
$[\pm 45/0/90]_s$	39.0	120	31.9	29.6	3.4	32.8
AS4/3501-6						
$[\pm 45/0_3]_s$	38.7	99.6	32.2	29.8	34.9	28.4
$[90/0/\pm 45/0]_s$	40.1	113	32.5	29.8	0.5	36.7
$[\pm 45/0/90]_s$	39.2	121	32.1	29.6	5.0	32.1

It can be seen in Table. 3 that the resulting frequencies show the same trends as presented in Table. 2. That is, the highest increment of frequency is the 2nd mode for all laminates except the 5th mode with the following stacking sequences: $[\pm 45/0/90]_s$ and $[90/0/\pm 45/0]_s$.

6. Summary

In this work, the composite rotor blades made of S2Glass/Epoxy, Kev49/Epoxy and AS4/3501-6 with the symmetrical stacking sequences were developed and analyzed by finite element method. Due to the interest in low frequency, the resulting frequencies of the first 6 modes consisting of three flapwise modes, two edgewise modes and one torsion mode were extracted. To study the effect of constraint, the additional boundary condition was applied. The results revealed that the supplementary boundary condition attached away from the rotor hub at the ratio $L / \Delta_1 = 13.25$ and $L / \Delta_2 = 7.75$ respectively can cause the blade frequency shift. It is

interesting to note that the 2nd mode exhibits the significant increment of frequency for all three types of laminates as the frequency of the 5th mode is no more than 5% increase for the $[\pm 45/0/90]_s$ and $[90/0/\pm 45/0]_s$ laminates.

7. Acknowledgement

The author acknowledges the support by the Faculty of Engineering, King Mongkut's University of Technology North Bangkok, Thailand.

8. References

- [1] Bauchau, O.A. and Hong, C.H. (1987). Finite element approach to rotor blade modeling, *Journal of the American Helicopter Society*, vol. 32(1), January 1987, pp. 60-67.
- [2] Smith, E.C. and Chopra, I. (1991). Formulation and evaluation of an analytical model for composite box beam, *Journal of the American Helicopter Society*, vol. 36(3), 1991, pp. 23-35.
- [3] Cesnik, C.S. and Hodges, D.H. (1997). VABS: A new concept for composite rotor blade cross-sectional modeling, *Journal of the American Helicopter Society*, vol. 42(1), January 1997, pp. 27-37.
- [4] Jung, S.N., Nagaraj, V.T. and Chopra, I. (1999). Assessment of composite rotor blade modeling techniques, *Journal of the American Helicopter Society*, vol. 44, July 1999, pp. 188-205.
- [5] Yu, W. (2007). Efficiency high - fidelity simulation of multibody systems with composite dimensionally reducible components, *Journal of the American Helicopter Society*, vol. 52, January 2007, pp. 49-57.
- [6] Rice, C.G. and Zepler, E. (1967). Loudness and pitch sensation of an impulsive sound of very short duration, *Journal of Sound and Vibration*, vol. 5(2), 1967, pp. 285-289.

- [7] Jakobsen, J. (2005). Infrasound emission from wind turbine, *Journal of Low Frequency Noise, Vibration and Active Control*, vol. 24(3), 2005, pp. 145-155.
- [8] Leventhall, G. (2006). Infrasound from wind turbines: fact, fiction or deception, *Journal of Canadian Acoustics*, vol. 34(2), 2006, pp. 29-36.
- [9] Pedersen, E. and Persson, W.K. (2007). Wind turbine noise, annoyance and self-reported health and well-being in different living environments, *Journal of Occupational and Environmental Medicine*, vol. 64(7), 2007, pp. 480-6.
- [10] Chandrupatla, T.R. and Belegundu, A.D. (2002). *Introduction to Finite Elements in Engineering*, Prentice Hall, New Jersey.
- [11] Rao, S.S. (1995). *Mechanical Vibrations*, Addison-Wesley, New York.
- [12] Sun, C.T. (2007). *Mechanics of Composite Materials and Laminates*, Purdue University, Indiana.
- [13] Herakovich, C.T. (1998). *Mechanics of Fibrous Composites*, John Wiley & Sons, New York.
- [14] Simulia Inc. (2010). *ABAQUS 6.9 Manual*, Providence, Rhode Island.